Accepted Manuscript

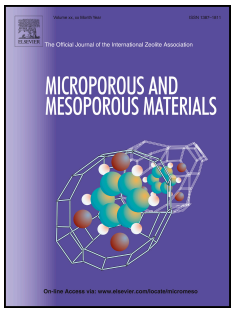

Visible light absorption of surface modified TiO_2 powders with bidentate benzene derivatives

B. Milićević, V. Đorđević, D. Lončarević, S.P. Ahrenkiel, M.D. Dramićanin, J.M. Nedeljković

PII: S1387-1811(15)00355-8

DOI: 10.1016/j.micromeso.2015.06.028

Reference: MICMAT 7187

To appear in: *Microporous and Mesoporous Materials*

Received Date: 9 March 2015

Revised Date: 11 June 2015

Accepted Date: 23 June 2015

Please cite this article as: B Milićević, V Đorđević, D Lončarević, S. Ahrenkiel, M. Dramićanin, J. Nedeljković, Visible light absorption of surface modified TiO_2 powders with bidentate benzene derivatives, *Microporous and Mesoporous Materials* (2015), doi: 10.1016/j.micromeso.2015.06.028.

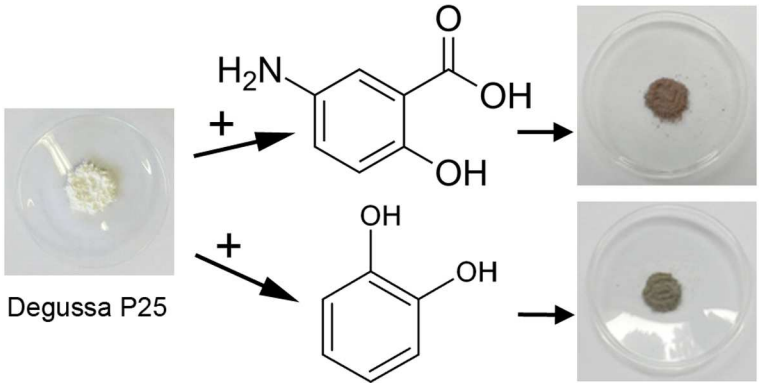

Visible light absorption of surface modified TiO_2 powders with bidentate benzene derivatives

B Milićević[a], V Đorđević[a], D Lončarević[b], S P Ahrenkiel[c], M D Dramićanin[a] and J M Nedeljković[a,*]

[a] Vinča Institute of Nuclear Sciences, University of Belgrade, P.O. Box 522, 11001 Belgrade, Serbia

[b] Institute of Chemistry, Technology and Metallurgy, University of Belgrade, Department of Catalysis and Chemical Engineering, Njegoševa 12, 11 000 Belgrade, Serbia

[c] South Dakota School of Mines & Technology, Rapid City, South Dakota, USA

*Corresponding author email: jovned@vinca.rs

Abstract

TiO_2 powders with different specific surface area were prepared using reproducible, sol-gel synthetic route and their ability to form hybrids with catechol and 5-amino salicylic acid was compared with the commercially available Degussa P25 TiO_2 powder. Microstructural characterization involving transmission electron microscopy, X-ray diffraction analysis and nitrogen adsorption-desorption isotherms indicated that TiO_2 samples cover reasonably wide size and/or specific surface area range (50-115 m^2/g). The surface modification of TiO_2 powders with catechol and 5-amino salicylic acid induced significant shift of absorption to the visible spectral region due to charge transfer complex formation. It should be emphasized that tunable optical properties of TiO_2 in powder form have never been reported in the literature. The largest red

shift of the absorption onset was observed for sample with the largest specific surface area upon surface modification with both ligands. The binding of the modifier molecules to the surface Ti atoms was studied using Fourier transform infrared spectroscopy.

Key-words: TiO_2, sol-gel, surface modification, catechol, 5-amino salicylic acid

1 Introduction

Titanium dioxide (TiO_2) is one of the most studied semiconductors suitable for use in heterogeneous catalysis [1,2], photocatalysis [3,4], solar cells [5], production of hydrogen, ceramics, electric devices, as well as white pigment, corrosion-protective coatings, gas sensors [6], etc. Also, TiO_2 nanoparticles deposited on textile fibers show antibacterial and self-cleaning activities [7,8]. Recently, new approaches for creating and utilizing bioinorganic composites of nanoscale TiO_2 have been extensively investigated for biomedical applications [9]. It is well known that the bulk TiO_2 material appears in three major crystal phases: rutile (tetragonal), anatase (tetragonal) and brookite (rhombohedral). Rutile is a high temperature stable phase and has band gap energy of 3.0 eV (415 nm), while the anatase formed at a lower temperature with band gap energy of 3.2 eV (387 nm), and refractive index of 2.3, is common in fine-grained (nanoscale) natural and synthetic samples [10]. Due to its large band gap, TiO_2 absorbs less than 5 % of the available solar photons. There has been tremendous interest in recent years to improve visible light absorption of TiO_2, including dye sensitization for photoexcitation of TiO_2 in the visible spectral region via photoinduced interfacial electron transfer [11–13], and doping with light and heavy elements to promote less

energetic excitations of electrons from mid-gap dopant levels to conduction band of TiO_2 [14–16]. Another emerging approach involves a charge transfer from surface modifier into the conduction band of nanocrystalline TiO_2 particles. This type of binding is considered to be exclusive for colloidal TiO_2 particles in the nanocrystalline domain due to change of the coordination of Ti surface atoms from octahedral to square-pyramidal [17,18]. So far, charge-transfer complex (CTC) formation accompanied with red shift of absorption onset up to 1.3 eV has been reported for colloidal TiO_2 nanoparticles surface modified with either catecholate- or salicylate-type of ligands [19–23].

For a variety of applications, it is more desirable to use materials in powder form instead of colloidal solutions, and attempt was made to obtain spherical submicron TiO_2 powder particles in the aerosol-assisted processing of precursor TiO_2 colloids [24,25]. Although submicron TiO_2 particles were successfully modified with different ligands (ascorbic acid, dopamine, catechol, 2,3-dihydroxynaphthalene and anthrarobin) providing absorption in visible spectral range, main drawback of this synthetic approach lies in the fact that is time and energy consuming, and gives a low yield.

This study is continuation of our efforts to improve light absorption of TiO_2 powders by extending the absorption spectrum into the red, and making TiO_2 functional over a more practical range of solar spectrum. The simplicity of the surface modification of TiO_2 in powder form and their ability to form hybrids with catechol (CAT) and 5-amino salicylic acid (5-ASA) is the main advantage of the presented approach. For that purpose, the commercial photocatalyst Degussa P25 and TiO_2 nano-powders, prepared using highly reproducible low cost sol-gel synthetic route, were studied. Thorough microstructural characterization of synthesized TiO_2 nano-powders involving

transmission electron microscopy, X-ray diffraction analysis and nitrogen adsorption-desorption isotherms indicated that the chosen samples cover a reasonably wide size and/or specific surface area range. Special attention was paid to the optical properties of surface modified TiO_2 powders. Reflection spectroscopy was used for optical characterization of surface modified TiO_2 powders, while infra-red spectroscopy was used in order to understand coordination of CAT and 5-ASA to surface Ti atoms.

2 Experimental

2.1 Synthesis of TiO_2 nano-powders

The incorporation of Eu^{3+} ions into TiO_2 nanocrystals was performed using hydrolytic sol-gel route described elsewhere [26]. Briefly, for the synthesis of TiO_2 nanopowder doped with 1.0 at.% of Eu^{3+} ions, titanium(IV) isopropoxide (Alfa Aesar, 95%), water, ethanol (JT Baker, HPLC grade) and nitric acid (JT Baker, 69.0–70.0%) were mixed at a molar ratio of 1:3:20:0.08. In the first step, 5.9 ml of titanium(IV) isopropoxide was dissolved in 23.3 ml of ethanol under constant stirring. Next, 0.1056 g of Eu_2O_3 was dissolved into 0.11 ml of concentrated HNO_3 and diluted with 1.1 ml of water. The obtained solution was added to titanium(IV) isopropoxide/ethanol mixture. Transparent gels were obtained within a few minutes at room temperature in air atmosphere. Then gels were dried at 70 °C for 5 h. The dried gels were transferred to crucibles and heated at a rate of 5 °C/min to a final temperature of 210 °C and held at that temperature for 20 min. Finally, samples were calcinated at 420 °C for 2 h. Undoped TiO_2 nano-powder was prepared in the same manner as TiO_2:Eu^{3+}

nano-powder keeping exactly the same molar ratio between titanium(IV) isopropoxide, water, ethanol and nitric acid. The commercially available TiO_2 powder (Degussa P25) was used as received.

2.2 Surface modification of TiO_2 powders with catechol and 5-amino salicylic acid

Surface modification of Degussa P25, TiO_2 and TiO_2:Eu^{3+} was performed by dispersing 0.1 g of powder in 10 ml of water containing either 22.0 mg of CAT or 30.6 mg of 5-ASA; molar ratio between any of TiO_2 powders and ligands (CAT and 5-ASA) was 6.25:1. Formation of CTC was indicated by immediate coloration of dispersion. Mixture was left overnight and after that surface-modified TiO_2 powders were separated by centrifugation, washed several times with a water/ethanol mixture in order to remove excess ligands, and finally dried at 40 °C in the vacuum oven for 24 h.

2.3 Characterization

Transmission electron microscopy (TEM) was performed using a JEOL JEM-2100 LaB6 instrument operated at 200 kV. TEM images were acquired with a Gatan Orius CCD camera at 2× binning.

X-ray diffraction (XRD) powder patterns were recorded using Rigaku SmartLab instrument under the Cu $K\alpha_{1,2}$ radiation. The intensity of diffraction was measured with continuous scanning at 2º/min. The data were collected at 0.02º intervals.

Nitrogen adsorption-desorption isotherms were determined on Sorptomatic 1990 Thermo Finnigan automatic system using nitrogen physisorption at -196 ºC. Before

measurement the samples were outgassed at 130 ºC for 3 h. Specific surface area of the samples (S_{BET}) was calculated from the nitrogen adsorption-desorption isotherms according to the Brunauer, Emmett and Teller (BET) method [27]. Pore size distribution was estimated by applying Barret, Joyner and Halenda (BJH) method [28] to the desorption branch of isotherm.

Optical properties of TiO_2 powders, as well as surface modified TiO_2 powders with CAT and 5-ASA were studied in UV-Vis spectral range by diffuse reflectance measurements (Thermo Nicolet Evolution 500 spectrometer equipped with diffuse reflectance accessory).

Diffuse reflectance infrared spectra of TiO_2 powders, CAT and 5-ASA, as well as surface modified TiO_2 powders with CAT and 5-ASA were measured using a Thermo Nicolet 6700 FTIR spectrometer with a Collector II Diffuse Reflectance Accessory at spectral resolution of 8 cm^{-1} in the region of 4000-400 cm^{-1}.

3 Results and Discussion

3.1 Microstructural characterization of TiO_2 and TiO_2:Eu^{3+} powders

Representative TEM images at high magnification of TiO_2 and TiO_2:Eu^{3+} powders are presented in Figure 1 (A and B, respectively). Both powders have similar morphology, and consist of loosely agglomerated nanoparticles with irregular, rounded and rectangular shapes, and variable dimensions. Detailed inspection of TiO_2 and TiO_2:Eu^{3+} samples showed the presence of well-crystallized TiO_2 nanoparticles without irregularities or amorphous surface layers, and with similar sizes. Slightly reduced average size, from 13.6 to 7.3 nm, was induced by doping TiO_2 nanoparticles with Eu^{3+}

ions at concentration level as low as 1 at.%. This result is in agreement with literature data concerning inhibition of crystal growth upon doping of TiO_2 with rare-earth elements [29,30]. Analysis of the selected area electron diffraction (SAED) patterns of both TiO_2 samples (see insets to Figures 1A and 1B) revealed prominent diffraction rings consistent with the anatase crystal structure, including 101, 103, 004, 112, 200, 105, 211 and 204. Microstructural characteristics (phase composition, particle size, specific surface area, porosity) of Degussa P25 powder are well-known, and described elsewhere [31–33]. For the sake of clarity, this data are presented in Table 1, together with data obtained for undoped and doped TiO_2 powders prepared by sol-gel synthetic route.

The XRD patterns of TiO_2 and TiO_2:Eu^{3+} nano-powders are shown in Figure 2 (curves (a) and (b), respectively). Both patterns consists of the characteristic, intense peaks at 25.3, 37.8, 48.0, 53.9, 55.1, and 62.1 degrees that correspond to 101, 004, 200, 105, 211 and 204 main reflections from anatase titania (JCPDS 00-021-1272). It should be mentioned that there is no indication of the presence of any other crystalline phase in both samples. The grain size, determined from the peak broadening and Scherrer's equation, was found to be 101 and 91 Å for TiO_2 and TiO_2:Eu^{3+} nano-powders, respectively. Thus, the grain sizes given by the XRD measurements are in agreement with the sizes of nanoparticles by TEM analysis of TiO_2 samples.

Nitrogen adsorption-desorption isotherms of synthesized TiO_2 and TiO_2:Eu^{3+} samples are shown in Figure 3A (curves (a) and (b), respectively). According to the IUPAC classification, isotherms of both TiO_2 powders belong to type IV with a hysteresis loop associated to mesoporous materials. The shape of hysteresis loop is of type H2 which indicates poorly defined pore shapes. Specific surface areas calculated by the BET

equation were found to be 88 and 114 m^2g^{-1} for TiO_2 and TiO_2:Eu^{3+} powders, respectively. It should be noticed that specific surface areas of both synthesized samples are higher compared to commonly used commercial Degussa P25 TiO_2 powder (50-60 m^2g^{-1}) [31–33]. Pore size distribution of undoped and doped TiO_2 samples are shown in Figure 3B (curves (a) and (b), respectively). It is clear that both, undoped and doped TiO_2 powders are mesoporous with the pore diameter of 6.4 and 3.6 nm, respectively.

As mentioned earlier, microstructural characteristics of synthesized TiO_2 and TiO_2:Eu^{3+} powders, as well as commercial Degussa P25 powder are collected in Table 1. Obtained data using TEM, XRD and nitrogen adsorption isotherms are in good agreement. The results showed that samples differ significantly, indicating that the chosen samples cover a reasonably wide size and/or specific surface area range.

3.2 Surface modification of Degussa P25, TiO_2 and TiO_2:Eu^{3+} powders with CAT and 5-ASA

Appearance of brawn color upon treatment of Degussa P25, TiO_2 and TiO_2:Eu^{3+} powders with CAT and 5-ASA indicated red shift in the absorption onset of surface modified TiO_2 powders compared to the unmodified ones. Kubelka–Munk transformations of UV-Vis diffuse reflection data of unmodified TiO_2 powders and surface modified TiO_2 powders with CAT and 5-ASA are shown in Figure 4. In the case of unmodified TiO_2 samples (Degussa P25, TiO_2 and TiO_2:Eu^{3+} powders synthesized by sol-gel technique), a steep rise of absorption can be observed in UV spectral range bellow 400 nm (Figure 4A), corresponding to the band gap energy of anatase (3.2 eV). Bumps at 2.67 and 2.32 eV, observed upon Kubelka–Munk transformations of diffuse

reflection data from TiO_2:Eu^{3+} powder belong to $^5D_2 \rightarrow {}^7F_0$ and $^5D_1 \rightarrow {}^7F_0$ transitions of Eu^{3+} dopant ions, respectively [34].

On the other hand, surface modification with CAT (Figure 4B) and 5-ASA (Figure 4C) induced significant red shift of optical absorption of Degussa P25, as well as TiO_2 and TiO_2:Eu^{3+} powders synthesized by sol-gel technique (curves (a), (b) and (c) in Figures 4B and 4C, respectively). For comparison, reflection spectra of free ligands (CAT and 5-ASA) in powder form are also included in Figures 4B and 4C, respectively. Coordination of CAT and 5-ASA to the sample with the largest specific surface area (TiO_2:Eu^{3+} powder) induced the largest red shift of optical absorption (peaks were found to be around 1.9 eV (≈650 nm) in both cases). It should be noticed that TiO_2 powders with smaller specific surface area (Degussa P25 and TiO_2 powder prepared by sol-gel route) surface modified with CAT and 5-ASA have two peaks/shoulders whose position does not depend on the specific surface area. Peaks/shoulders in low energy part of the spectra upon surface modification of all TiO_2 powders with both ligands are placed at almost the same position (≈1.9 eV). On the other hand, surface modified Degussa P25 and TiO_2 powder prepared by sol-gel route have peaks in high-energy spectral region whose positions are slightly different depending on used ligand (around 2.8 and 3.0 eV for 5-ASA and CAT, respectively). It seems that the increase of the low-energy peak takes place at the expense of the high energy peak upon CTC formation between TiO_2 powder with the highest specific surface area and CAT or 5-ASA. Due to increased background absorption ranging from 400 to 800 nm, it is difficult to determine the values for absorption onset upon surface modification of TiO_2 powders. The red absorption shift due to CTC formation is roughly estimated to be at least 1.3 eV.

It should be emphasized that CTC formation and consequent red shift of optical absorption after surface modification of commercial Degussa P25 TiO_2 powder with the same/similar ligands has not been previously reported in the literature. So far, the optical changes were observed for small (less than 20 nm) TiO_2 nanospheres [17,19–23], submicron TiO_2 spheres obtained using nanometer in size TiO_2 colloids as a precursor in the aerosol-assisted processing [24, 25], and commercially available sodium trititanate ($Na_2Ti_3O_7$) nanotubes with outer diameters of 5–8 nm and lengths of 50–500 nm [35].

The significant change of effective band gap energy of small TiO_2 nanoparticles was assigned to the formation of CTC between electron-donating ligands and coordinately unsaturated Ti atoms at the surface. It is well known that, in the nanosize regime, due to the large curvature of TiO_2 particles, the coordination of surface Ti atoms changes from octahedral to square-pyramidal [17,18]. Binding of electron-donating ligands to coordinately unsaturated Ti atoms simultaneously restores their coordination to octahedral geometry and changes the electronic properties of a TiO_2 semiconductor [36]. As a consequence, absorption of light by the CTC promotes electrons from the chelating ligand directly into the conduction band of TiO_2 nanocrystallites, resulting in the red shift of the semiconductor absorption compared to unmodified nanocrystallites [17]. The importance of this finding – that the CTC formation between Degussa P25 and catecholate- or salicylate-type of ligands takes place – lies in the indication that tunable optical properties are not exclusively characteristics of small TiO_2 particles with distorted coordination of surface Ti atoms, but, rather a general phenomenon, occurring, under proper conditions, with commercially available, larger than 20 nm TiO_2 particles. In addition, surface modification, followed with red shift of optical absorption, was

achieved with mesoporous TiO_2 and TiO_2:Eu^{3+} powders consisting of nanoparticles smaller than 20 nm, prepared using sol-gel route involving high-temperature treatment for several hours. So far, the CTC formations with the same/similar ligands have been reported in literature for colloidal TiO_2 nanoparticles prepared in a different way (acidic hydrolysis of $TiCl_4$) [17,19–23]. Sol-gel synthesis, as a robust and simple approach, provides an easy way to produce a larger quantity of material in comparison to the colloidal route.

Having in mind that the main purpose of extending the absorption spectrum of TiO_2 into the red spectral region is usage of less energetic photons to drive photo-induced reactions, preliminary/row data concerning photocatalytic performance of surface modified Degussa P25 powder with CAT are presented in Supplement 1. Photocatalytic ability of red-shifted TiO_2 powder was tested under visible light illumination by following the degradation of organic dye crystal violet. The low energy band-pass 450 nm cut-off filter was used to eliminate photons with energy higher than 2.75 eV. The preliminary results clearly indicate that surface modified Degussa P25 powder with CAT is able to photocatalytically perform under visible light illumination. The level of enhancement of redox chemistry in red-shifted TiO_2 powders by taking advantage of electron promotion from the ground state of CTC into the conduction band of TiO_2 will be the subject of our detailed study.

FTIR spectroscopy measurements were performed to elucidate the mechanism for binding of CAT and 5-ASA to the surface of TiO_2 powders. Because the infrared spectrum of TiO_2 powder has only the characteristic broadband in 3700–2000 cm^{-1} spectral region [37], we were able to measure surface-modified TiO_2 powders in 1700–1000 cm^{-1} spectral region, where the characteristic bands of ligands exist. The FTIR

spectra of CAT and 5-ASA, free and bound to the surface of commercial TiO_2 powder (Degussa P25) are presented in Figures 5A and 5B, respectively. The FTIR spectra of surface modified TiO_2 powders, prepared using sol-gel synthetic approach, are almost the same as the FTIR spectra of surface modified Degussa P25 powder, and for the sake of clarity are not shown.

The main bands and their assignment [38–40] in free CAT (Figure 5A, curve a) are as follows: stretching vibrations of aromatic ring ν(C–C)/ν(C=C) at 1624, 1605, 1530 and 1475 cm^{-1}, stretching vibrations of the phenolic group ν(C–OH) at 1288, 1266 and 1250 cm^{-1}, bending vibrations of the phenolic group δ(C–OH) at 1374, 1201, 1169 and 1150 cm^{-1}, and bending vibrations of δ(C–H) at 1100 and 1043 cm^{-1}. Upon adsorption of CAT onto TiO_2 particles (Figure 5A, curve (b)), the difference between FTIR spectra of free and adsorbed ligands appears, indicating surface complexation with CAT bound to the oxide surface. All bands associated with the bending vibrations of the phenolic group δ(C–OH) completely disappeared, indicating the binding of CAT to TiO_2 via two adjacent phenolic groups. The binding of CAT to TiO_2 via two adjacent phenolic groups affects the stretching vibrations of the aromatic ring and stretching vibrations of the phenolic group, followed with disappearance of all bands with exception of bands at 1485 and 1261 cm^{-1}. The binding of CAT onto colloidal TiO_2 nanoparticles (4.5 nm), whose surface Ti atoms are coordinately unsaturated was reported to result in the formation of bidentate binuclear bridging complexes [19,20]. Having in mind that commercial TiO_2 particles (Degussa P25) are larger than the critical size necessary for development of unsaturated coordination of surface Ti atoms and that the rutile phase is also present, formation of monodentate chelating complexes cannot be rule out.

The FTIR spectrum of free 5-ASA (Figure 5B, curve (a)) is in agreement with literature data [41,42]. The main bands in free (protonated) acid can be assigned [43–51] to overlapping stretching vibrations of the C=O of the carboxyl group with stretching vibration of amino group at 1666 cm^{-1}, stretching vibrations of the aromatic ring ν(C-C)/ν(C=C) at 1506 and 1471 cm^{-1}, bending vibrations of the phenolic group δ(C-OH) at 1389, 1365 and 1250 cm^{-1}, stretching vibration of amino group at 1316 and 1272 cm^{-1} and bending δ(C–H) vibrations at 1193, 1139 and 1088 cm^{-1}. The adsorption of 5-ASA onto TiO_2 powder (Figure 5B, curve (b)) leads to the almost complete disappearance of the bands at 1506, 1471, 1389, 1365 and 1250 cm^{-1}. Since these bands correspond to vibrations of the phenolic and carboxylic groups, it is obvious that both groups take part in the chelation of titanium atoms. The appearance of bands at 1379/1350 and 1575 cm^{-1} that can be attributed to carboxylate symmetric and asymmetric stretching vibrations [44,45], respectively, prove the deprotonation of the COOH group as a consequence of its binding to Ti atoms with the formation of the delocalized carboxylate group [52,53]. It should be mentioned that the adsorption of 5-ASA onto TiO_2 powder even affected bending δ(C–H) vibrations at 1193, 1139 and 1088 cm^{-1}, and induced their complete disappearance. On the other hand, vibrations that belong to amino group can be observed upon adsorption of 5-ASA onto TiO_2 powders at slightly shifted positions (1656, 1291 and 1256 cm^{-1}). Having in mind reactivity of amino group [54], its availability might be important for synthesis of more complex systems.

4 Conclusions

The abilities of commercially available Degussa P25 TiO_2 powder, as well as undoped TiO_2 powder, and TiO_2 powder doped with 1.0 at.% of Eu^{3+} ions, prepared using reproducible sol-gel synthetic route, to form CTCs with catechol and 5-amino salicylic was tested. Thorough microstructural characterization of TiO_2 samples was performed indicating reasonable wide size and/or specific surface area range (50-115 m^2/g). On the other hand, chosen modifiers (CAT and 5-ASA) represent typical catecholate- or salicylate-type of ligands. The binding of the modifier molecules to surface Ti atoms induced significant shift of absorption to the visible spectral range due to CTC formation. The extent of red shift, as well as a way of binding of the modifier molecules to the surface Ti atoms, for all studied TiO_2 powders, is similar to literature data concerning colloidal TiO_2 nanoparticles with distorted coordination of Ti surface atoms from octahedral to square-pyramidal. The CTC formation between Degussa P25 and catecholate- or salicylate-type of ligands indicates that tunable optical properties are not exclusive for small TiO_2 particles with distorted coordination of surface Ti atoms. Adjustment of optical properties of commercially available TiO_2 powders or custom-made TiO_2 powders provides the possibility to extend this type of research from entirely fundamental to more applicable. Investigation of photocatalytic performance of surface modified TiO_2 powders is underway in our laboratories. The preliminary results, using degradation of organic dye crystal violet as a test reaction, indicated that red-shifted TiO_2 powders have photocatalytic activity under the illumination with photons whose energy is smaller than 2.75 eV.

Acknowledgement

Financial support for this study was granted by the Ministry of Education, Science and Technological Development of the Republic of Serbia (Project 45020).

References

[1] A.L. Linsebigler, G. Lu, J.T. Yates Jr., Chem. Rev. 95 (1995) 735–758.

[2] A.O. Ibhadon, P. Fitzpatrick, Catalysts 3 (2013) 189–218.

[3] M.R. Hoffmann, S.T. Martin, W. Choi, D.W. Bahnemann, Chem. Rev. 95 (1995) 69–96.

[4] U. Stafford, K.A. Gray, P.V. Kamat, Heterogen. Chem. Rev. 3 (1996) 77–104.

[5] B. O'Regan, M. Grätzel, Nature 353 (1991) 737–740.

[6] X. Chen, S.S. Mao, Chem. Rev. 107 (2007) 2891–2959.

[7] D. Mihailović, Z. Šaponjić, R. Molina, N. Pauč, P. Jovančić, J. Nedeljković, M. Radetić, ACS Appl. Mater. Inter. 2 (2010)1700–1706.

[8] D. Mihailović, Z. Šaponjić, M. Radoičić, S. Lazović, C.J. Baily, P. Jovančić, J. Nedeljković, M. Radetić, Cellulose 18 (2011) 811–825.

[9] T. Rajh, N.M. Dimitrijevic, M. Bissonnette, T. Koritarov, V. Konda, Chem. Rev. 114 (2014) 10177–10216.

[10] T.K. Kim, M.N. Lee, S.H. Lee, Y.C. Park, C.K. Jung, J.H. Boo, Thin Solid Films 475 (2005) 171–177.

[11] I. Martini, J. Hodak, G.V. Hartland, P.V. Kamat, J. Chem. Phys. 107 (1997) 8064–8072.

[12] S.Y. Huang, G. Schlichthörl, A.J. Nozik, M. Grätzel, A.J. Frank, J. Phys. Chem. B 101 (1997) 2576–2582.

[13] R.J. Ellingson, J.B. Asbury, S. Ferrere, H.N. Ghosh, J.R. Sprague, T. Lian, A.J. Nozik, J. Phys. Chem. B 102 (1998) 6455–6458.

[14] E. Barborini, A.M. Cont, I. Kholmanov, P. Piseri, A. Podesta, P. Milani, C. Cepek, O. Sakho, R. Macovez, M. Sancrotti, Adv. Mater. 17 (2005) 1842–1846.

[15] M. Chiodi, C.P. Cheney, P. Vilmercati, E. Cavaliere, N. Mannella, H.H. Weitering, L. Gavioli, J. Phys. Chem. C 116 (2011) 311–318.

[16] M.V. Dozz, E. Selli, J. Photochem. Photobiol. C 14 (2013) 13–28.

[17] T. Rajh, J.M. Nedeljković, L.X. Chen, O. Poluektov, M.C. Thurnauer, J. Phys. Chem. B 103 (1999) 3515–3519.

[18] L.X. Chen, T. Rajh, W. Jäger, J. Nedeljković, M.C. Thurnauer, J. Synchrotron Rad. 6 (1999) 445–447.

[19] I.A. Janković, Z.V. Šaponjić, M.I. Čomor, J.M. Nedeljković, J. Phys. Chem. C 113, (2009) 12645–12652.

[20] I.A. Janković, Z.V. Šaponjić, E.S. Džunuzović, J.M. Nedeljković, Nanoscale Res. Lett. 5 (2010) 81–88.

[21] T.D. Savić, I.A. Janković, Z.V. Šaponjić, M.I. Čomor, D.Ž. Veljković, S.D. Zarić, J.M. Nedeljković, Nanoscale 4 (2012) 1612–1619.

[22] T.D. Savić, Z.V. Šaponjić, M.I. Čomor, J.M. Nedeljković, M.D. Dramićanin, M.G. Nikolić, D.Ž. Veljković, S.D. Zarić, I.A. Janković, Nanoscale 5 (2013) 7601–7612.

[23] T.D. Savić, M.I. Čomor, J.M. Nedeljković, D.Ž. Veljković, S.D. Zarić, V.M. Rakić, I.A. Janković, Phys. Chem. Chem. Phys. 16 (2014) 20796–20805.

[24] I.M. Dugandžić, D.J. Jovanović, L.T. Mančić, N. Zheng, S.P. Ahrenkiel, O.B. Milošević, Z.V. Šaponjić, J.M. Nedeljković, J. Nanopart. Res. 14 (2012) 1157–1167.

[25] I.M. Dugandžić, D.J. Jovanović, L.T. Mančić, O.B. Milošević, S.P. Ahrenkiel, Z.V. Šaponjić, J.M. Nedeljković, Mater. Chem. Phys. 143 (2013) 233–239.

[26] Ž. Antić, R. Krsmanović, M.G. Nikolić, M. Marinović-Cincović, M. Mitrić, S. Polizzi, M.D. Dramićanin, Mater. Chem. Phys. 135 (2012) 1064–1069.

[27] S. Brunauer, P.H. Emmett, E. Teller, J. Am. Chem. Soc. 60 (1938) 309–319.

[28] E.P. Barret, L.G. Joyner, P.P. Halenda, J. Am. Chem. Soc. 73 (1951) 373–380.

[29] M. Borlaf, S. Caes, J. Dewalque, M.T. Colomer, R. Moreno, R. Cloots, F. Boschini, Thin Solid Films 558 (2014) 140–148.

[30] J. Reszczyńska, T. Grzyb, J.W. Sobczak, W. Lisowski, M. Gazda, B. Ohtani, A. Zaleska, Appl. Surf. Sci. 307 (2014) 333–345.

[31] C.B. Almquist, P. Biswas, J. Catal. 212 (2002) 145–156.

[32] K.J.A. Raj, B. Viswanathan, Indian J. Chem. 48A (2009) 1378–1382.

[33] K. Suttiponparnit, J. Jiang, M. Sahu, S. Suvachittanont, T. Charinpanitkul, P. Biswas, Nanoscale Res. Lett. 6 (2011) 27.

[34] J-C.G. Bünzli, S.V. Eliseeva, in: P. Hänninen, H. Härmä (Eds.), Lanthanide Luminescence, Springer Berlin Heidelberg, 2011, pp. 1–45.

[35] D. Jaušovec, M. Božič, J. Kovač, J. Štrancar, V. Kokol, J. Colloid Interf. Sci. 438 (2015) 277–290.

[36] P. Persson, R. Bergström, S. Lunell, J. Phys. Chem. B 104 (2000) 10348–10351.

[37] T. Rajh, L.X. Chen, K. Lukas, T. Liu, M.C. Thurnauer, D.M. Tiede, J. Phys. Chem. B 106 (2002) 10543–10552.

[38] P.A. Connor, K.D. Dobson, A.J. McQuillan, Langmuir 11 (1995) 4193–4195.

[39] P.Z. Araujo, C.B. Mendive, L.A. Garcia Rodenas, P.J. Morando, A.E. Regazzoni, M.A. Blesa, D. Bahnemann, Colloid Surf. A 265 (2005) 73–80.

[40] P.Z. Araujo, P.J. Morando, M.A. Blesa, Langmuir 21 (2005) 3470–3474.

[41] C.Y. Panicker, H.T. Varghese, A. John, D. Philip, K. Istvan, G. Keresztury, Spectrochim. Acta A 58 (2002) 281–287.

[42] K. Zou, H. Zhang, X. Duan, Chem. Eng. Sci. 62 (2007) 2022–2031.

[43] J. H. S. Green, W. Kynaston, A.S. Lindsey, Spectrochim. Acta 17 (1961) 486–502.

[44] E.C. Yost, M.I. Tejedor-Tejedor, M.A. Anderson, Environ. Sci. Technol. 24 (1990) 822–828.

[45] S. Tunesi, M.A. Anderson, Langmuir 8 (1992) 487–495.

[46] B. Humbert, M. Alnot, R. Quilès, Spectrochim. Acta A 54 (1998) 465–476.

[47] A.D. Weisz, L.G. Rodenas, P.J. Morando, A.E. Regazzoni, M.A. Blesa, Catal. Today 76 (2002) 103–112.

[48] L. Jiang, L. Gao, Y. Liu, Colloids Surf. A 211 (2002) 165–172.

[49] X. Guan, G. Chen, C. Shang, J. Environ. Sci. 19 (2007) 438–443.

[50] B. Rusch, K. Hanna, B. Humbert, Environ. Sci. Technol. 44 (2010) 2447–2453.

[51] G. Socrates, Infrared and Raman characteristic group frequencies, third ed., Wiley, New York, 2001.

[52] M.V. Biber, W. Stumm, Environ. Sci. Technol. 28 (1994) 763–768.

[53] E.M. Cooper, D. Vasudevan, J. Colloid Interface Sci. 333 (2009) 85–96.

[54] S. Mourdikoudis, L.M. Liz-Marzán, Chem. Mater. 25 (2013) 1465–1476.

Table 1. Comparison of phase composition, size, specific surface area and pore diameter of TiO_2 powders used in this study

	Degussa P25	TiO_2	TiO_2:Eu^{3+}
Phase	80% anatase and 20% rutile[a]	Pure anatase	Pure anatase
Particle Size (TEM) [nm]	26[a] 30[b]	13.6±2.3	7.3±2.7
Grain Size (XRD) [nm]	21[a] 27[c]	10.1	9.1
Specific Surface Area (BET) [m^2/g]	50[b] 56[a] 57.4[c]	87.9	114.4
Pore Diameter (BJH) [nm]	17.5[a]	6.4	3.6

[a]Ref. 32
[b]Ref. 31
[c]Ref. 33

Figure captions

Figure 1. TEM data from TiO_2 powders: typical TEM image of TiO_2 powder (A), and 1.0 at.% Eu^{3+} doped TiO_2 powder (B) at high magnification; insets: corresponding SAED patterns.

Figure 2. XRD patterns of undoped (a), and 1 at.% Eu^{3+} doped TiO_2 (b) powders; the most pronounced reflections are indexed according to JCPDS card no. 21-1272 (anatase TiO_2).

Figure 3. (A) Nitrogen adsorption isotherms of undoped (a) and 1 at.% Eu^{3+} doped TiO_2 (b) powders. (B) BJH pore size distribution of undoped (a) and 1 at.% Eu^{3+} doped TiO_2 (b) powders.

Figure 4. Kubelka-Munk transformations of diffuse reflection data for Degussa P25 (curves a), TiO_2 (curves b), and TiO_2:Eu^{3+} (curves c) powders: (A) as prepared/received, (B) surface modified with CAT, and (C) surface modified with 5-ASA. Reflection spectra of free ligands (CAT and 5-ASA) in powder form are included in B and C, respectively.

Figure 5. (A) FTIR spectra of free CAT (a), and CAT adsorbed on Degussa P25 TiO_2 powder (b). (B) FTIR spectra of free 5-ASA (a), and 5-ASA adsorbed on Degussa P25 TiO_2 powder (b).

Supplement 1. Photocatalytic ability of Degussa P25 powder surface modified with CAT (Kubelka-Munk transformation of the reflection spectrum of red shifted TiO_2 powder is given as inset to Supplement 1) was studied using the degradation of organic dye crystal violet (CV). The photocatalytic reactions were induced using Osram Vitalux lamp (300 W). The low energy band pass 450 nm cut-off filter was used to exclude UV part from the illumination light (transmission spectrum of the cut-off filter is given as inset to Supplement 1). Concentration of photocatalyst was 2 mg/mL, while initial concentration of CV was 11.5 μM. Absorption spectra of initial CV solution and after

equilibration in dark with red shifted Degussa P25 powder are given by black and red lines, respectively. Absorption spectra of CV after 1.5 and 3.0 hours of illumination with visible light are given by green and blue lines, respectively.

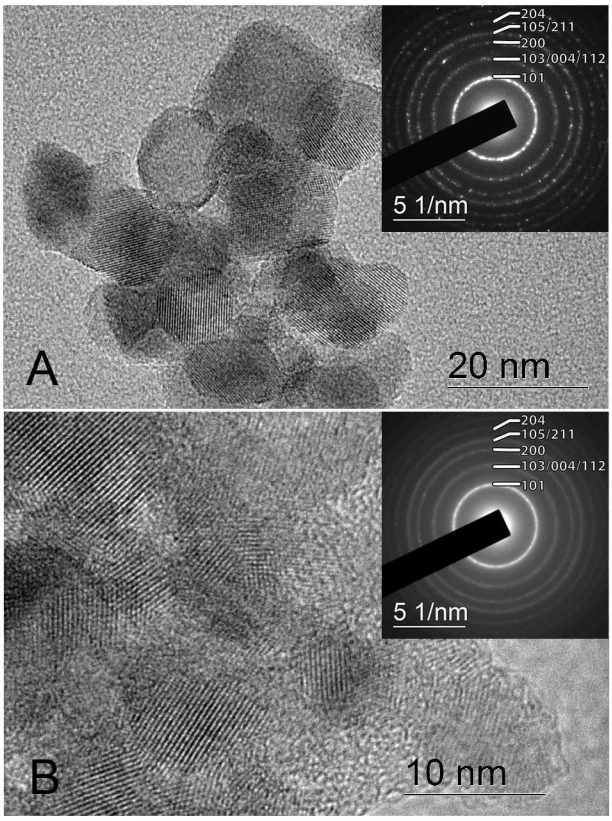

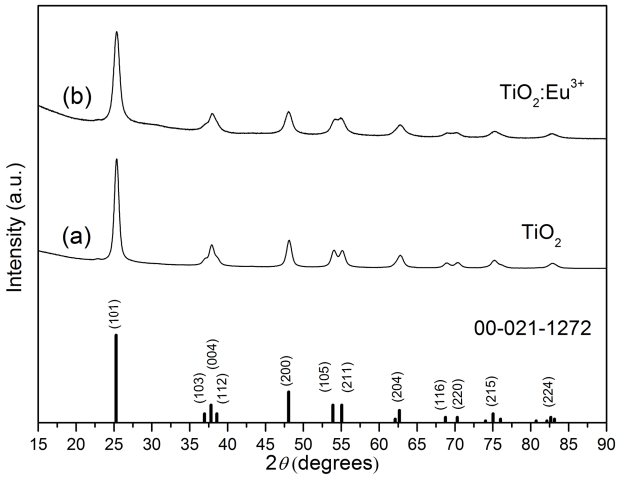

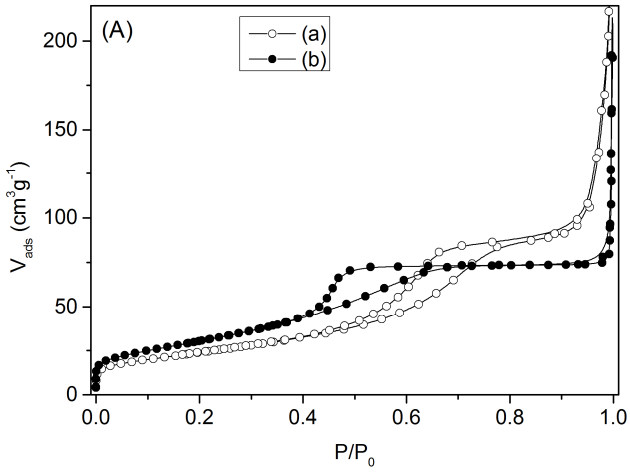

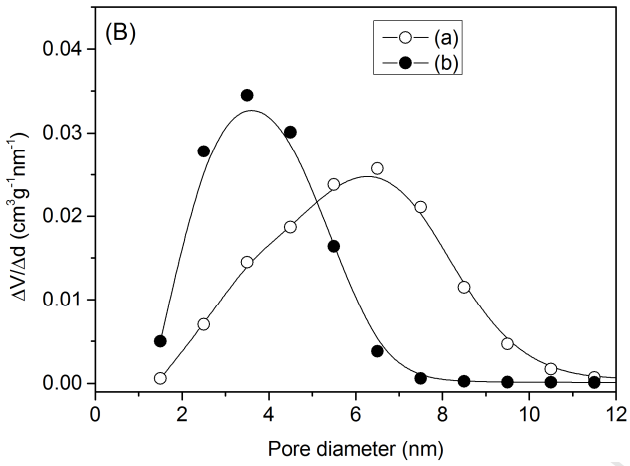

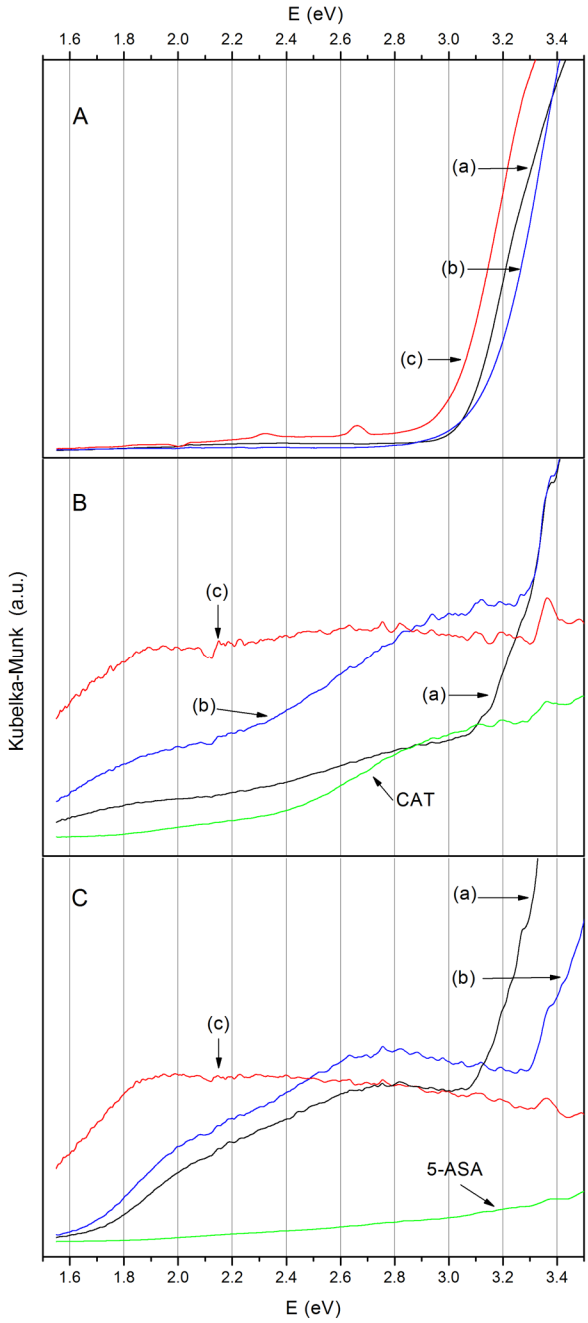

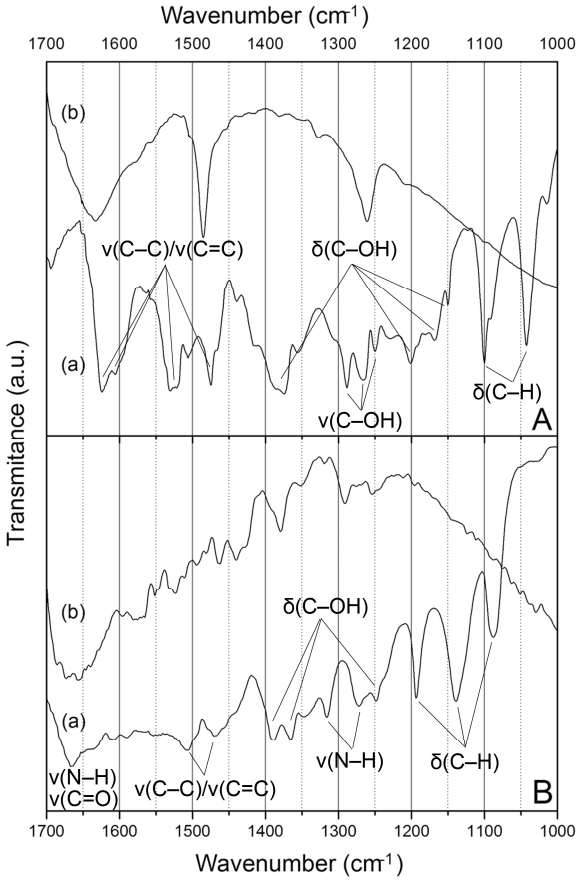

Highlights

- Adjustment of optical properties of commercial and mesoporous TiO_2 powders
- Charge transfer complex formation between surface Ti atoms and benzene derivatives
- Extent of absorption in visible proportional to the specific surface area of TiO_2
- Tunable optical properties are not exclusive for “small” TiO_2 particles